Science of the Total Environment 947 (2024) 174421

Contents lists available at ScienceDirect

Science of the Total Environment

journal homepage: www.elsevier.com/locate/scitotenv

Regional differences in the impact paths of climate on aboveground biomass in alpine grasslands across the Qinghai-Tibet Plateau

Peixian Li [a,b,d], Wenquan Zhu [c,d,*], Bangke He [c,d]

[a] ASEAN-China Satellite Remote Sensing Application Centre (Ocean Remote Sensing Center), Fourth Institute of Oceanography, Ministry of Natural Resources, Beihai 536000, China
[b] Guangxi Key Laboratory of Beibu Gulf Marine Resources, Environment and Sustainable Development, Fourth Institute of Oceanography, Ministry of Natural Resources, Beihai 536000, China
[c] State Key Laboratory of Remote Sensing Science, Beijing Normal University, Beijing 100875, China
[d] Beijing Engineering Research Center for Global Land Remote Sensing Products, Faculty of Geographical Science, Beijing Normal University, Beijing 100875, China

HIGHLIGHTS

- The impact paths of climate and phenology on AGB were unveiled at the regional scale.
- Climate primarily affected variations in alpine grassland AGB via direct paths.
- Water and heat accumulation during the growing season boosted AGB consistently.
- Water and heat accumulation had opposing impacts on AGB in temperate arid regions.

GRAPHICAL ABSTRACT

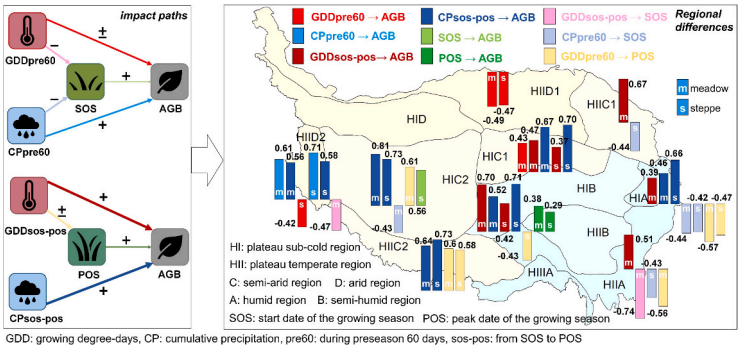

GDD: growing degree-days, CP: cumulative precipitation, pre60: during preseason 60 days, sos-pos: from SOS to POS

ARTICLE INFO

Editor: Zhaozhong Feng

Keywords:
Aboveground biomass
Alpine grasslands
Impact paths
Water and heat accumulation
Phenology

ABSTRACT

Alpine grasslands on the Qinghai-Tibet Plateau (QTP) play an essential role in water conservation, biodiversity protection and climate feedback, with aboveground biomass (AGB) serving as a crucial indicator of grassland health and functionality. While previous studies have independently explored the phenological differences, cumulative effects, and spatial variability of climatic impacts on biomass/productivity in alpine grasslands, the cascading effects regarding climate and phenology on AGB still present knowledge gaps. Here, using peak AGB measurements, remote sensing and gridded climate data in the QTP alpine grasslands during 2002–2018, we systematically analyzed the impact paths of climatic variables (i.e., cumulative precipitation, CP; growing degree-days, GDD) and phenology-mediated paths (start and peak date of the growing season, SOS and POS) on AGB and their regional differences. During the preseason (pre60) or the growing season (sos-pos), climate primarily directly impacted variations in AGB across different climatic regions, although a phenology-mediated path by which climate indirectly affected AGB existed (i.e., GDDsos-pos → POS → AGB). Three general patterns were revealed: In the plateau temperate arid regions, an increase in CPpre60 significantly promoted AGB (path coefficients $w = 0.61$–0.71), whereas an increase in GDDpre60 inhibited AGB ($w = -0.42 \sim -0.49$); In the

* Corresponding author at: State Key Laboratory of Remote Sensing Science, Beijing Normal University, Beijing 100875, China.
E-mail address: zhuwq75@bnu.edu.cn (W. Zhu).

https://doi.org/10.1016/j.scitotenv.2024.174421
Received 22 April 2024; Received in revised form 26 June 2024; Accepted 29 June 2024
Available online 5 July 2024

plateau sub-cold regions, increases in both CPsos-pos and GDDsos-pos significantly promoted AGB, respectively (w = 0.46–0.81 and w = 0.37–0.70); Similarly, in the plateau temperate arid or semi-arid regions, increases in CPsos-pos also significantly promoted the AGB (w = 0.56–0.73). This study highlights that the water and heat accumulation mainly exert direct impacts on alpine grassland AGB across various climatic regions and phenological stages, providing insights into the mechanism driving AGB by climate and phenology during spring and summer.

1. Introduction

Grassland ecosystems encompass 37 % of the Earth's terrestrial surfaces and store approximately one-third of terrestrial carbon, which play a pivotal role in ecological services and security, carbon cycling processes and climate change mitigation (O'Mara, 2012; Scurlock and Hall, 1998; Bai and Cotrufo, 2022). Grasslands characterized by low productivity and water-limited are particularly susceptible to climatic disturbances and anthropogenic interventions (Knapp and Smith, 2001; Li, 2017; Wang et al., 2021; Du et al., 2022; Ma et al., 2022). As Earth's third pole, due to its severe cold, drought, and high-altitude environmental features, the Qinghai-Tibet Plateau (QTP) is highly sensitive to climate warming (Li, 2017; Zhang et al., 2019). The annual average warming linear rate (0.16 °C/10a) on the QTP surpassed that of the Northern Hemisphere during the period 1955–1996 (Liu and Chen, 2000). Especially, current research reported that the surface air temperature trend increased at a rate of 0.37 °C/10a on the QTP during 1961–2018, based on 82 observation stations (Zhang et al., 2023a). The alpine grasslands, predominant on the QTP, are essential for climate feedback, water conservation and biodiversity protection across East Asia (Wang et al., 2022b). These grasslands provide various ecological functions and services to plateau ecosystem consumers, including habitats, foods, medicinal herbs, water resource regulation, etc. (Fayiah et al., 2020; Dong et al., 2020). Additionally, they are essential production resources that bolster and enhance the livelihoods of pastoralists, underpinning the local livestock industry. To understand the impact of rapid climate change on alpine grasslands is of great significance for ecological protection and planning.

Aboveground biomass (AGB) refers to the dry weight of living plants that accumulates on the ground per unit area (g/m^2 or kg/ha) (Fang et al., 2001). As a crucial component of the carbon cycling and vegetation management in ecosystems, the AGB is intricately linked to plant-environment interactions and competitive strategies (Weiher et al., 1999; Rehling et al., 2021). Specifically, the dynamics of AGB are not only driven by a complex mix of abiotic factors including climatic and edaphic variables, but also modulated by plant functional traits such as phenology and height (Li et al., 2021b). Furthermore, the impact of climate on grassland biomass/productivity exhibited phenological differences and cumulative effects. On one hand, the temperatures during specific phenophases aligned more closely with actual requirements for vegetative growth than do annual average temperatures (Michaletz et al., 2014). Similarly, precipitation in the growing season had a more pronounced effect on vegetative AGB than annual precipitation, underscoring the critical influence of seasonal climate conditions (Hossain and Li, 2020). These phenophase-specific climatic drivers significantly enhance the predictability of both intra- and interannual biomass variations (Robinson et al., 2013). On the QTP, the temperature throughout various growth stages and soil moisture levels prior to the senescence stage were pivotal for the carbon sequestration capabilities of alpine grasslands (You et al., 2020). Notably, precipitation during the reproductive growth period (July–August) emerged as the most important controlling factor (Zhai et al., 2022). On the other hand, both immediate response and cumulative effects of temperature conditions have been observed in the growth patterns of subalpine plant species (Hoffmann et al., 2010). Given the explanation of climate cumulative effects on global vegetation dynamics was 68.33 %, which was approximately 11.27 % higher than considering only instantaneous climatic variables (Wen et al., 2019). At present, although the phenological differences and cumulative effects of climatic impact on biomass/productivity have been unveiled independently, the combined effects on alpine grassland biomass are yet to be fully understood, especially dividing phenophases and climate regions.

Due to the diverse terrain and varying climate across the QTP, differentiating climate regions is crucial for accurately assessing the impact of climate on grassland biomass (Wang et al., 2017). It was reported that the peak date of the growing season (POS), the Standardized Precipitation-Evapotranspiration Index (SPEI) and $NDVI_{max}$ showed high spatial heterogeneity across the QTP, generally, the higher drought, the more delayed the POS (ca. 57 %) (Li et al., 2020). The response of the start date of the growing season (SOS) and $NDVI_{max}$ to preseason snow cover varied among different climate regions, SOS was positively correlated with snow melt date in most areas on the QTP, whereas it was negatively correlated in the warm but drier areas (Wang et al., 2018b). Along elevational gradients and across distinct climate regions, the relative contribution of climate factors to the alpine grassland productivity/biomass was also spatially heterogeneous. The productivity in the southwestern QTP was more sensitive to temperature than precipitation and radiation (Li et al., 2019). Therefore, segmenting the QTP into different climate regions emerges as an effective strategy to elucidate the complex impacts of climatic variables on the biomass in alpine grasslands.

Currently, many researches primarily focuses on the climate direct impacts on biomass (Wang et al., 2017; Li et al., 2019). A few site-scale studies have explored phenology-mediated effects on biomass (i.e., climate → phenology → productivity/biomass). For instance, Ganjurjav et al. (2021) investigated the climate-indirect impact paths on alpine meadows biomass through mediating the SOS or EOS (End date of the growing season) based on warming and precipitation addition control experiments on the QTP. Novelly, alpine meadow (*Kobresia pygmaea*) can offset the negative effects of climate warming on biomass by adjusting the SOS. According to eight flux sites, Koebsch et al. (2020) reported solar radiation mainly directly affected peatlands gross ecosystem productivity (GEP) in European, while temperature indirectly affected GEP by acting on the SOS or EOS. Exploring the climate-impact paths on grassland biomass is expected to uncover the mechanisms of biomass variation. To our knowledge, the carbon accumulation during the advancement of spring phenology might continue to promote summer vegetation growth through the 'snowball effect', known as the "vegetation growth carryover" (Ogle et al., 2015; Lian et al., 2021). Conversely, the accelerated vegetation growth can consume additional environmental resources needed for subsequent growth, potentially leading to an increase in biomass that exceeds the natural carrying capacity (e.g., soil water), thereby impeding vegetation growth in subsequent seasons, known as the "vegetation structural overshoot" (Jump et al., 2017). Importantly, in the QTP alpine grasslands, Chen et al. (2022) found that advanced spring phenology promoted spring vegetation productivity, which partially compensated for the decline in vegetation productivity caused by summer drought. However, the applicability of the two hypotheses mentioned hasn't been fully validated in QTP alpine grasslands across various climate regions. Additionally, the POS, as the date when the foliage area reaches the maximum value within the year, will affect the terrestrial carbon absorption in the peak growing season (Gonsamo et al., 2018). Compared with the generally focused SOS and EOS, the POS was less considered to

study the climate-impact path on grassland biomass.

Therefore, by dividing phenophases and climate regions, this study will extract climatic variables (cumulative precipitation and growing degree-days) and phenological indicators (SOS and POS), aiming to analyze the impact paths of climate on AGB and regional differences of these paths in the QTP alpine grasslands. Specifically, two aspects will be focused on: (i) at the regional scale, does climate indirectly impact AGB through phenological mediation? (ii) What are the regional differences in the paths of climatic and phenology-mediated impacts on AGB under different phenological stages? We expect to provide valuable insights into the regional-difference patterns to AGB driven by climate across the alpine grasslands, as well as examine the phenological effects on AGB variation during spring and summer. Furthermore, in the context of continued climate warming, the study anticipates establishing a foundation for predicting the trends in biomass variation, analyzing alterations in carbon fixation as well as protecting grassland resources in the Asian Water Tower (QTP).

2. Data and methods

2.1. Study area

The Qinghai-Tibet Plateau (QTP) is located in the southern part of the Asian continent, extends longitudinally from 73°18′52″E to 104°46′59″E and latitudinally from 26°00′12″N to 39°46′50″N. Spanning an area of 2.5 million km^2, the plateau boasts an average elevation exceeding 4000 m above sea level (Zhang et al., 2002). Grasslands constitutes approximately 54 to 70 % of the total QTP, mainly include alpine meadow and alpine steppe (Wang et al., 2022b). Recognized as one of the most dynamically interactive regions among Earth's spheres, the QTP presents a complex interplay of horizontal and vertical zonalities (Chen et al., 2019). Specifically, the QTP spans the gradients from arid to humid regions, encompassing subtropical to sub-cold regions, primarily influenced by the monsoon, atmospheric circulation and its significant elevational variation (Sun et al., 2022). The annual average temperature is about −2.5 °C and annual average precipitation is about 380 mm on the QTP (Wang and Chen, 2023). In this research, the study area is the intersection part of grasslands phenology, AGB and climate variables within the QTP. The HIIIA, HID and HIIB climate regions were excluded from the study because they didn't contain both meadow and steppe simultaneously (Fig. 1).

2.2. Data

2.2.1. Aboveground biomass data

Aboveground biomass data originated from the National Tibetan Plateau/Third Pole Environment Data Center (https://doi.org/10.11888/Terre.tpdc.272587; Zhang et al., 2023b). The dataset encompassed spatial data of AGB across the QTP during 2000–2019, with a resolution of 250 m. It investigated 906 pairs of on-site AGB samples and drone images from 2015 to 2019 (where grassland samples were cut and dried at 65 °C to a constant weight), and 2602 sets of Moderate-Resolution Imaging Spectroradiometer (MODIS) pixel-level drone data, comprising over 37,000 aerial images. Employing random forests and stepwise upscaling methods, the dataset was effectively upscaled from the traditional quadrat scale (0.5 m) to the MODIS image scale (250 m). Further, the high-precision regional AGB was obtained, with an estimated average R^2 of 0.83 and RMSE of 34.13 g/m^2. In this study, the grassland AGB refers to the aboveground stock of grasslands after removing litter and biological feeding amounts, representing the annual peak aboveground biomass.

2.2.2. Climatic and phenological data

Climatic data were sourced from the China Meteorological Forcing Dataset (CMFD), which includes daily average temperature and daily precipitation. The CMFD, notable for being China's first high spatial and temporal resolution gridded near-surface climate data, offers a spatial resolution of 0.1° and is available in three temporal resolutions: 3-h, daily and monthly (He et al., 2020). This dataset was driven by integrating observations from over 700 ground stations, augmented by remote sensing products and reanalysis datasets (He et al., 2020). Verification of on-site observation results demonstrated superior data quality compared to GLDAS (Global Land Data Assimilation System). Furthermore, a comparative analysis of six types of precipitation raster data across the QTP highlighted the CMFD's exceptional accuracy in capturing daily precipitation, particularly during the cold season (Zhang et al., 2022).

Grassland phenology data were derived using the MODIS V6 MOD09A1 reflectance product (see Section 2.3.1 for the extraction method), which offers 8-day composite data (500 m) with atmospheric correction for gases, aerosols, and Rayleigh scattering. To ensure compatibility and spatial analysis accuracy, climate and AGB data were resampled to a 500 m resolution.

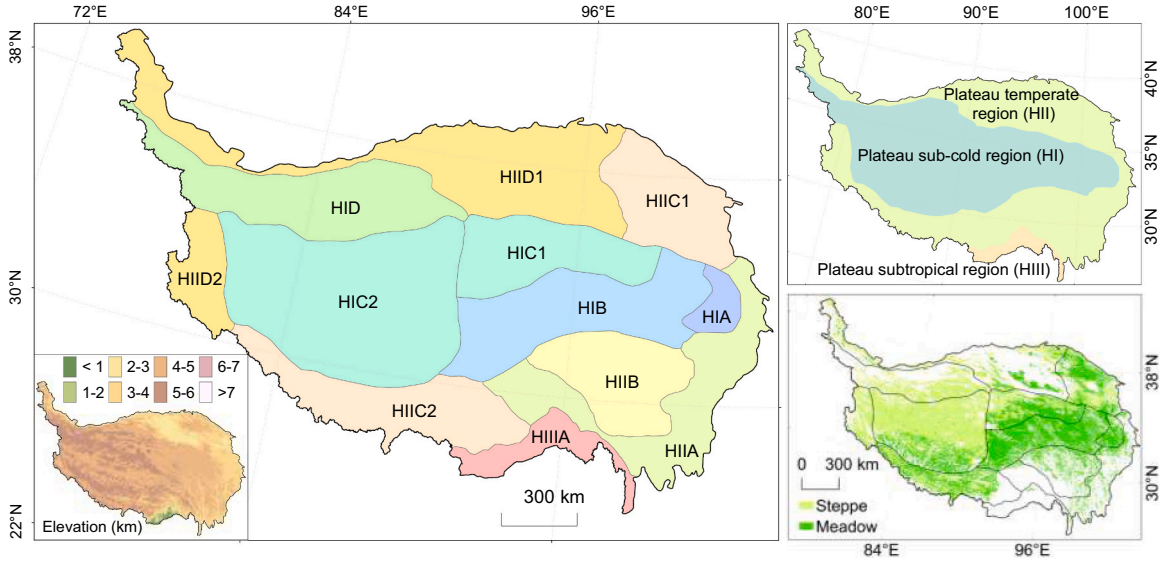

Fig. 1. Climate regions, grassland types, and elevation on the Qinghai-Tibet Plateau. The climate regions used for this study: plateau sub-cold region includes humid region (HIA), semi-humid region (HIB), semi-arid regions (HIC1, HIC2); plateau temperate region (HII) includes humid region (HIIA), semi-arid regions (HIIC1, HIIC2) and arid regions (HIID1, HIID2).

2.2.3. Ancillary data

The vegetation type map was obtained from the 1:1 million Vegetation Map of the People's Republic of China, compiled by the Chinese Vegetation Map Editorial Committee of the Chinese Academy of Sciences (2001). In this map, the two principal vegetation type groups in alpine regions—meadow and steppe—were extracted across the QTP. Among them, alpine meadows account for about 96 % of the meadow area, and alpine steppes account for about 85 % of the steppe area. Vegetation formation including *Kobresia capillifolia* alpine meodow, *Kobresia humilis* alpine meadow, *Kobresia setchwanensis* alpine meadow, *Stipa purpurea* alpine steppe, *Carex moorcroftii* alpine steppe, etc. The climate region map of the QTP was developed by vectorizing the simplified diagram from China's new scheme for climate regionalization (Zheng et al., 2010). Nine climate regions were identified from the climate divisions of the QTP, including two temperature regions, totaling four humid-arid regions (Fig. 1).

2.3. Methods

2.3.1. Phenological indicators extraction

Here, two phenological indicators were selected, including the start date of the growing season (SOS) and the peak date of the growing season (POS), to investigate their adjustments on AGB driven by climate. Considering the grassland spring phenology is strongly influenced by snow cover and snowmelt on the QTP, we utilized the background-free phenology index (BFPI) as proposed by Xie et al. (2022) to generate the SOS. The calculation formula is:

$$BFPI = NGSI \times NDGI \tag{1}$$

where NGSI is the Normalized Growing Season Index (Jolly et al., 2005), NDGI is the Normalized Difference Greenness Index (Yang et al., 2019b). Initially, the Growing Season Index (GSI) was calculated based on the minimum temperature, vapor pressure deficit and photoperiod (Jolly et al., 2005). Then, the GSI was normalized to derive the NGSI, which enhances the seasonal amplitude of the BFPI and improves model fitting. The NDGI reduces the impact of snow cover on phenology extraction by maximizing the contrast between vegetative and background information and minimizing changes in the reflectivity of background information (Yang et al., 2019b). According to formula (1), the BFPI inherits the characteristics of the non-growing season NGSI being zero and the advantages of the NDGI, thereby minimizing the interference from changes in non-growing season background information (such as snow, bare soil, and withered grass). Compared to the NGSI or single vegetation index, BFPI significantly enhances the accuracy of phenology extraction. Furthermore, BFPI also exhibits the superior precision in extracting SOS in grassland than in the other vegetation types such as deciduous broadleaf forest and evergreen broadleaf forest (Xie et al., 2022). Finally, we utilized a weighted double logistic function method to fit the BFPI time series data, and set a relative threshold of 10 % to extract the SOS (Zhu et al., 2022).

The extraction of POS followed three steps. Firstly, we performed cloud and snow removal using the quality files from MOD09A1 to generate time series of Enhanced Vegetation Index (EVI). Subsequently, the weighted double logistic function method was used to fit and reconstruct the EVI time series to mitigate abrupt declines in POS values. In regional evaluations, the method performed better than unweighted double logistic function fitting in retaining the original noise-free vegetation index and maximally recovering cloud pollution on the QTP (Zhu et al., 2022). Finally, we identified the day of the year (DOY) corresponding to the maximum value of the reconstructed EVI time series as the POS.

Furthermore, based on the SOS and POS extracted, two distinct phenophases were delineated (Fu et al., 2014; Shen et al., 2015; Gonsamo et al., 2018): First, termed the preseason 60 days, indicates the 60 days preceding the minimum SOS from 2002 to 2018 (SOS_{17min}). Second, defined as the growing season, spans from the maximum SOS (SOS_{17max}) to the minimum POS (POS_{17min}) over the same 17 years.

2.3.2. Climatic variables calculation

The calculation of climatic variables in the Qinghai-Tibet Plateau (QTP) area encompassed a detailed assessment of water and heat accumulation in alpine grasslands (meadows and steppes) during the defined preseason and growing season. This included calculating growing degree-days (GDD) (>0 °C) and cumulative precipitation (CP) based on average daily temperature and daily precipitation. The 60-day period was chosen for these calculations during the preseason because of the significant correlation between the SOS and the average temperature in the initial two to three months (Piao et al., 2006; Fu et al., 2014). Additionally, the strongest lagged response of cumulative precipitation on alpine grassland growth was observed within one to two months (Diao et al., 2021).

The calculation procedure for regional climate variables comprised several steps. Firstly, the SOS and POS pixel values for each year from 2002 to 2018 within the study area were calculated. Subsequently, for these 17 years, phenological extrema for each pixel were determined, including the minimum value at the start date of the growing season (SOS_{17min}), the maximum value at the start date of the growing season (SOS_{17max}) and the minimum value at the peak date of the growing season (POS_{17min}). The preseason 60 days and the growing season were calculated for each year's pixel according to the definition provided in Section 2.3.1. Lastly, water and heat accumulation values of each pixel for these phenological stages were computed in each year, encompassing the growing degree-days and cumulative precipitation during the preseason 60 days (GDDpre60, CPpre60) and growing season (GDDsos-pos, CPsos-pos), respectively. The calculation formulas are:

$$GDD = \sum_{DOY_1}^{DOY_2} \begin{bmatrix} (T_m - T_b)\ when\ \ T_m > T_b \\ 0\ when\ \ T_m \le T_b \end{bmatrix} \tag{2}$$

$$CP = \sum_{DOY_1}^{DOY_2} P \tag{3}$$

where the GDD (growing degree-days) refers to the cumulative sum of the differences between the T_m (daily average temperature) and the T_b (base temperature) from DOY_1 to DOY_2. T_b is set to 0 °C. The CP (cumulative precipitation) is the sum of precipitation at each phenological stage, and P is the daily precipitation. The DOY represents day of year. In the preseason, DOY_1 is the 60 days prior to the earliest start date of the growing season over the 17 years (SOS_{17min}), and DOY_2 is SOS_{17min} itself. During the growing season, DOY_1 is the latest start date of the growing season (SOS_{17max}), and DOY_2 is the earliest peak date of the growing season (POS_{17min}).

2.3.3. Path analysis

The path analysis is underpinned by the structural equation model (SEM) that uses a single indicator for each predictor variable without incorporating latent variables. Notably, piecewise structural equation modeling (pSEM) can estimate the dependent variable using small samples (Lefcheck, 2016). Specifically, this method decomposes the overall relationship of the dataset into simple or multiple linear regressions, assessing the coefficients and significance of each path separately. Subsequently, these results are integrated to formulate a global SEM (Shipley, 2000; Lefcheck, 2016). A significant advantage of pSEM is its flexibility with response variable distributions. It accommodates common distributions such as Bernoulli and Poisson without the prerequisite of normality. However, due to its inability to yield a valid global covariance matrix, pSEM necessitates an alternative approach for goodness-of-fit testing, namely Fisher's C (Shipley, 2000; Lefcheck, 2016):

$$C = -2\sum_{i=1}^{k} ln(P_i) \quad (4)$$

where C is the test statistic used in Fisher's method, which follows a chi-square distribution with 2 k degrees of freedom. P_i is the p-value from the i-th independence claim. An overall significance of model fit with a *P-value* > 0.05 indicates adequate modeling effectiveness. This study utilized the R package "piecewiseSEM" to implement pSEM testing (Lefcheck, 2016).

Before conducting path analysis, all variables were *Z*-score standardized (Li et al., 2021b; Wu et al., 2023). Then, the initial models were constructed by pSEM as shown in Fig. 2, and significance tests were performed for each path coefficient. Among these, "$p < 0.01$" indicated a high significance level, "$0.01 \leq p < 0.05$" indicated significance level. Due to the small sample size ($n = 17$), "$0.05 \leq p < 0.1$" was used to represent marginal significance. Based on meeting the overall index (Fisher's C: $P > 0.05$, Table S1, Table S2), the initial models gradually eliminated insignificant paths ($p > 0.1$), and simultaneously assessed the impact of each path' elimination on the Akaike information criterion (AIC) and Bayesian information criterion (BIC) (Ganjurjav et al., 2021). The optimal model was selected based on the minimum AIC and BIC values and the maximum coefficient of determination (R^2).

2.3.4. Processing flow

In the flowchart of the analytical methods, there were four blocks: data (input), phenological indicators extraction, climatic variables calculation and path analysis (Fig. 2). Detailed calculation processes for these can be found from Sections 2.3.1–2.3.3.

In the path analysis block, we first calculated regional spatial mean of the pixels within each climate region to ensure robustness in the representation of path indicators (Fig. 2). Second, when establishing the impact path, we considered the chronological principle: earlier events affect later events, which can explain why the climate variables during the post-growing season (from POS to EOS) are unlikely to affect peak AGB in the same year. The paths through which climate impacts phenology and AGB align with the physiological and ecological mechanisms of vegetation (Hoffmann et al., 2010; Fu et al., 2014; Chen et al., 2016; Gonsamo et al., 2018; Ganjurjav et al., 2021; Koebsch et al., 2020; Li et al., 2021b; Chen et al., 2022). For example, the transition of plant activity from peak season to spring in temperate ecosystems reflects an increase in carbon uptake (Gonsamo et al., 2018) (i.e., POS → AGB). The preseason hydrothermal variations could promote or inhibit the AGB accumulation during early spring (Zheng et al., 2020) (i.e., GDDpre60 → AGB, CPpre60 → AGB). Third, when validating the conceptual model, the direct and indirect paths through which climate affected AGB were examined based on the pSEM (Fig. 2, Fig. 3). Among them, the codes (1) and (2) represent indirect impact paths (Fig. 3), wherein the growing degree-days or cumulative precipitation in the preseason 60 days indirectly affected AGB through the SOS. Conversely, the code (5) represents direct impact path, where GDDpre60 or CPpre60 exerted a direct effect on AGB.

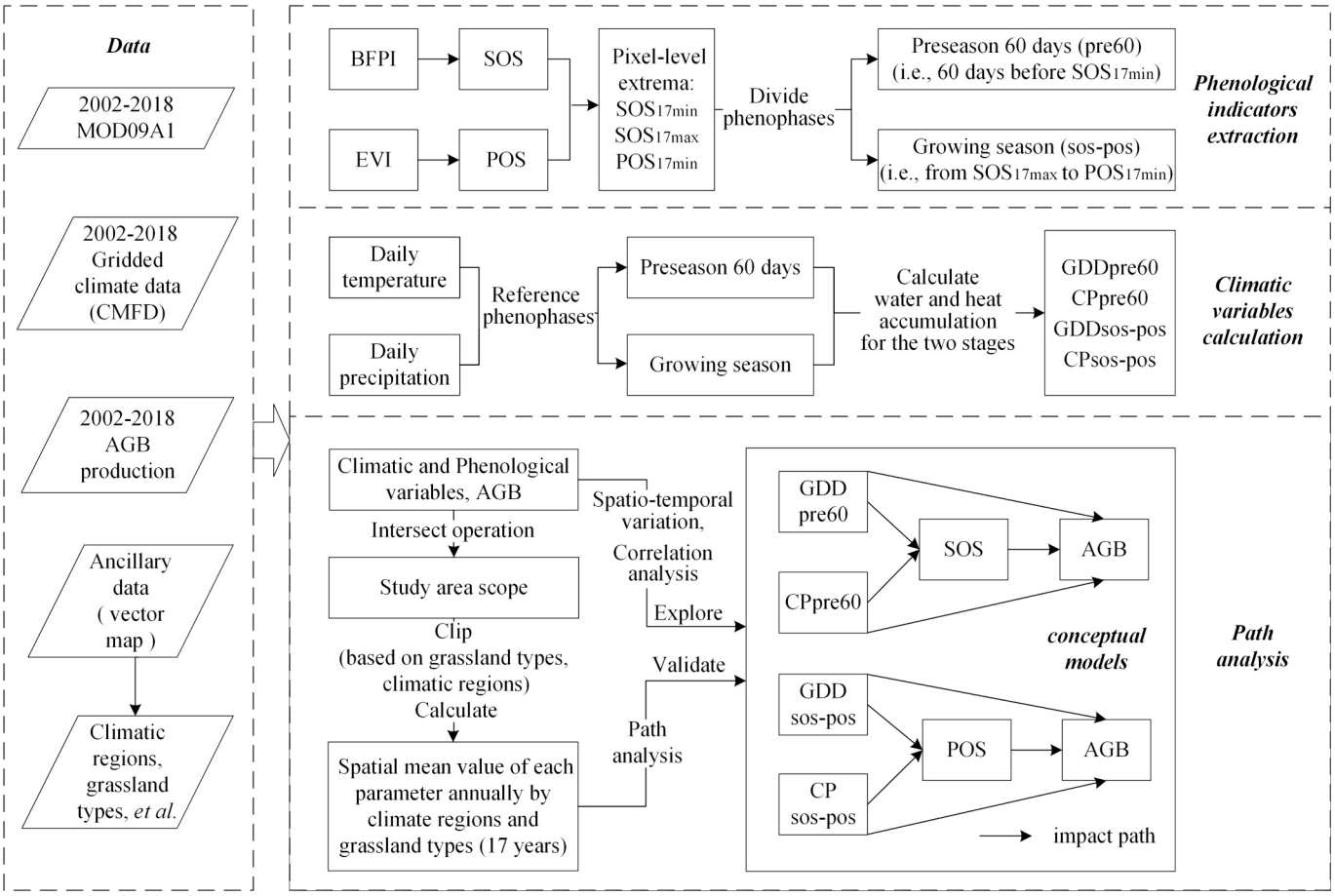

Fig. 2. Technical flowchart. AGB, aboveground biomass; BFPI, background-free phenology index; EVI, enhanced vegetation index; SOS, start date of the growing season; POS, peak date of the growing season. CPpre60 and GDDpre60 indicate the cumulative precipitation and growing degree-days during the preseason 60 days, respectively. CPsos-pos and GDDsos-pos indicate the cumulative precipitation and growing degree-days from SOS_{17max} to POS_{17min} (i.e., growing season).

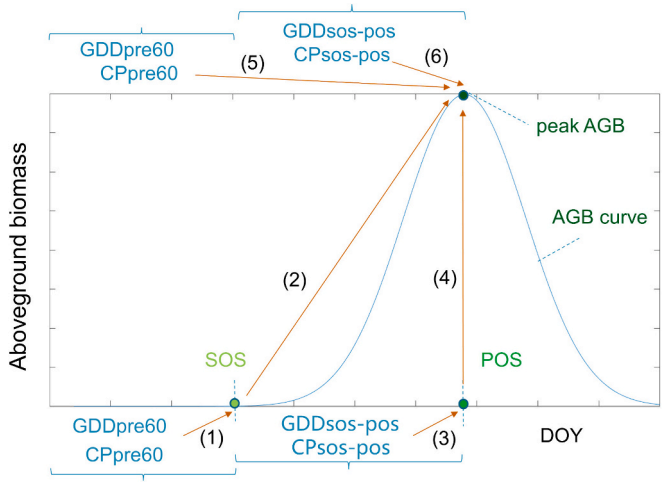

Fig. 3. Direct and indirect paths of climatic impact on AGB. AGB, aboveground biomass; SOS, start date of the growing season; POS, peak date of the growing season. CPpre60 and GDDpre60 indicate the cumulative precipitation and growing degree-days during the preseason 60 days, respectively. CPsos-pos and GDDsos-pos indicate the cumulative precipitation and growing degree-days from SOS_{17max} to POS_{17min} (i.e., growing season).

3. Results

3.1. Characteristics of aboveground biomass, phenology, and climate variables along climatic region gradients

The spatial distribution of multi-year average AGB in alpine grasslands exhibited a gradual decrease from the northeast to the southwest during 2002–2018 (Fig. S1). Approximately 19.5 % of the pixels showed AGB levels ranging from 2000 to 2500 kg/ha, predominantly situated in the plateau sub-cold humid region (HIA). About 47.2 % of the pixels fell within the range of 1500 to 2000 kg/ha, mainly located in the sub-cold semi-humid region (HIB). Pixels with AGB levels of 1000 to 1500 kg/ha and <1000 kg/ha accounted for 25.0 % and 8.2 %, respectively, extending from the northeast to the southwest on the QTP.

After dividing the climate regions, the multi-year average AGB exhibited a gradual decrease from the humid to arid regions during 2002–2018 (Fig. 4a). Across the moisture gradient in the plateau sub-cold regions (HIA, HIB, HIC1, HIC2, from humid to semi-arid), average AGB values declined progressively (Fig. 4a). Specifically, meadows registered AGB averages of 2129 ± 38 kg/ha (multi-year average ± standard deviation), 1746 ± 48 kg/ha, 1343 ± 91 kg/ha, 1138 ± 74 kg/ha, respectively; steppes reported 2143 ± 66 kg/ha, 1655 ± 76 kg/ha, 1189 ± 97 kg/ha, 1015 ± 62 kg/ha, respectively. Similar characteristics also occur in the temperate regions of the plateau (Fig. 4a). Additionally, meadows typically exhibited higher AGB than steppes, except in the sub-cold humid region (HIA) (Fig. 4a).

Across the entire QTP, the multi-year average spatial distribution of the SOS and POS in alpine grasslands also showed an overall delay from humid to arid regions (Fig. 4b, c, Fig. S2). In the sub-cold regions (HIA, HIB, HIC1, HIC2), the average SOS values for meadows were at DOY 131 ± 4, 155 ± 2, 160 ± 3, and 162 ± 4, respectively, and the averages of steppes were at DOY 135 ± 4, 153 ± 2, 161 ± 3, and 162 ± 4, respectively (Fig. 4b). The average POS for meadows occurred at DOY 214 ± 3, 220 ± 3, 222 ± 3 and 225 ± 5, respectively; steppes showed average POS values were at DOY 217 ± 4, 221 ± 3, 222 ± 4 and 225 ± 3, respectively. The similar change characteristics also occur in the plateau temperate regions (Fig. 4b, c). Exceptionally, along the moisture gradients, the SOS and POS in the temperate arid region (HIID1) displayed an anomalous advancement relative to other temperate regions.

The spatial-temporal variations in growing degree-days of the preseason 60 days (GDDpre60) mainly showed the differences between the

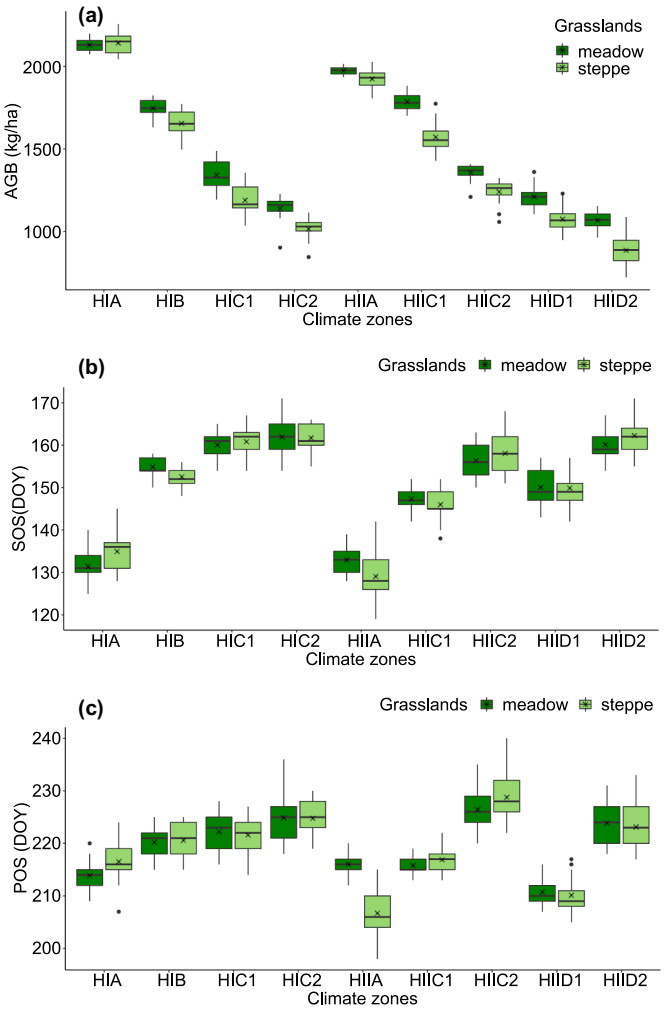

Fig. 4. Boxplot of multi-year averages of aboveground biomass and phenology in various QTP climate regions from 2002 to 2018 (the upper and lower horizontal lines of the box represent the 25–75 % confidence interval of the variable, and the black line and black cross in the box represent the median and average, respectively. In this study, the plateau sub-cold region includes the humid region (HIA), sub-humid region (HIB), sub-arid regions (HIC1, HIC2); the plateau temperate region (HII) includes the humid region (HIIA), sub-arid regions (HIIC1, HIIC2), and arid regions (HIID1, HIID2). AGB, aboveground biomass; SOS, start date of the growing season; POS, peak date of the growing season).

sub-cold and temperate regions (Fig. 5a, Fig. S3). The multi-year average GDDpre60 in the temperate regions (150 °C ± 55) was higher than that in the sub-cold regions (89 °C ± 23). Additionally, GDDpre60 varied significantly within similar moisture conditions across the two temperature regions. For example, in the temperate semi-arid regions (HIIC1, HIIC2), the average GDDpre60 of meadows and steppes were 102 ± 17 °C and 155 ± 25 °C, 157 ± 28 °C and 203 ± 31 °C, respectively. Conversely, in the sub-cold semi-arid regions (HIC1, HIC2), the GDDpre60 of meadows and steppes were only 63 ± 12 °C and 67 ± 11 °C, 102 ± 19 °C and 94 ± 18 °C, respectively.

The average of GDDsos-pos generally showed a gradual decrease from humid to arid regions (Fig. 5c, Fig. S4). In the sub-cold regions (i.e., HIA, HIB, HIC1, HIC2), the average GDD of meadows were 552 ± 41 °C, 340 ± 33 °C, 308 ± 38 °C, 296 ± 28 °C, respectively; and the average GDD of steppes were 541 ± 39 °C, 387 ± 36 °C, 295 ± 35 °C, 340 ± 27 °C, respectively. The similar GDDsos-pos change also occur in the plateau temperate regions.

The average of CPpre60 also presented a decreasing characteristic

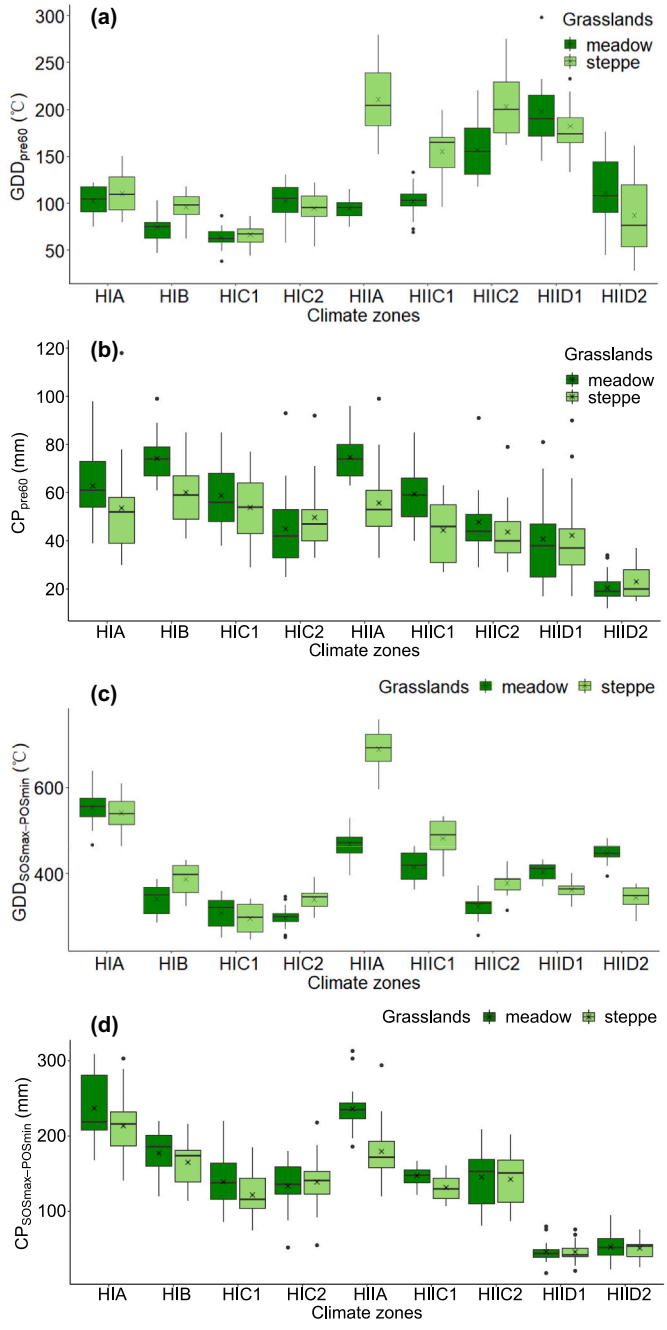

Fig. 5. Boxplot of multi-year average of water and heat accumulation along the climatic gradients during 2002–2018 (GDDpre60, growing degree-days in the preseason 60 days; CPpre60, cumulative precipitation in the preseason 60 days; $GDDsos_{max\text{-}pos_{min}}$, growing degree-days in the growing season, $CPsos_{max\text{-}pos\text{-}min}$, cumulative precipitation in the growing season).

along the moisture gradient (Fig. 5b, Fig. S3). Specifically, in the sub-cold regions (i.e., HIA, HIB, HIC1, HIC2), the average CPpre60 values of meadow were 63 ± 16 mm, 74 ± 10 mm, 59 ± 13 mm, 45 ± 17 mm, respectively; for steppes, the values were 54 ± 21 mm, 60 ± 13 mm, 54 ± 12 mm, 50 ± 15 mm, respectively. Consistently, in the temperate regions (i.e., HIIA, HIIC1, HIIC2, HIID1, HIID2), meadows exhibited average CPpre60 values of 75 ± 10 mm, 59 ± 12 mm, 48 ± 15 mm, 41 ± 18 mm and 21 ± 6 mm, respectively, and steppes showed average values of 56 ± 17 mm, 44 ± 12 mm, 44 ± 13 mm, 42 ± 19 mm, 23 ± 7 mm, respectively. Last but not least, the multi-year average CPsos-pos also exhibited a decreasing trend along these moisture gradients in the two temperature regions (Fig. 5d, Fig. S4).

3.2. The climate-impact paths on AGB at the climatic region scale

In the two phenophases, the indicators assessing the climate-impact paths on AGB were detailed in Table S1 to Table S2. During the growing season, the influence of climate on AGB was more pronounced compared to that in the preseason 60 days (as evidenced by the model coefficients in Tables S1 ~ S2). In addition, the paths through which climate impacts AGB did not clearly differ between meadows and steppes (Fig. 6).

3.2.1. Direct or indirect paths through which climate impacts on AGB

Overall, across the two phenophases, cumulative precipitation and growing degree-days predominantly exhibited a direct impact on AGB whether in the plateau sub-cold regions or temperate regions. However, a phenology-mediate indirect impact path was identified exclusively in the sub-cold semi-humid region (HIB). To be specific, the cumulative precipitation in the growing season negatively impacted the POS, and subsequently had a positive effect on AGB (i.e., GDDsos-pos $\overset{w_1}{\rightarrow}$ POS $\overset{w_2}{\rightarrow}$ AGB, path coefficient $w_1 = -0.43$, $w_2 = 0.29$, $p < 0.1$) (Fig. 6).

3.2.2. The paths and degree of climate impact on phenology in alpine grasslands

In the preseason 60 days, cumulative precipitation (CPpre60) negatively affected SOS across various regions ($p < 0.1$), not only including the plateau temperate regions (HIIA, steppe: $w = -0.43$; HIIC1, meadow: $w = -0.44$), but also the plateau sub-cold regions (HIA, meadow: $w = -0.44$, steppe: $w = -0.42$; HIC2, steppe: $w = -0.43$). During the growing season, the GDDsos-pos in the humid or semi-humid regions negatively affected the POS (HIA, meadow: $w = -0.56$, $p < 0.05$; HIIA, meadow: $w = -0.56$, $p < 0.05$), etc. In contrast, the GDDsos-pos positively impacted the POS in semi-arid regions (HIC2, meadow: $w = 0.61$, $p < 0.05$; HIIC2, meadow: $w = 0.60$, $p < 0.05$), et al. (Fig. 6c, d).

3.2.3. The path and degree of climate impact on AGB in alpine grasslands

In the preseason 60 days, cumulative precipitation (CPpre60) directly and positively affected the alpine grassland AGB in temperate arid regions (e.g., HIID2, steppe: $w = 0.71$, $p < 0.001$; HIID2, meadow: $w = 0.61$, $p < 0.01$). Nevertheless, GDDpre60 showed a directly negative effect on AGB in the temperate arid region, including the HIID1 (steppe: $w = -0.47$, $p < 0.1$; meadow: $w = -0.49$, $p < 0.05$) and HIID2 (meadow: $w = -0.42$, $p < 0.05$) (Fig. 6b). During the growing season, both GDDsos-pos and CPsos-pos strongly positively impacted AGB in almost all sub-cold regions. Among them, overall, the impact magnitude of CPsos-pos on AGB ($w = 0.46$–0.81, $p < 0.05$) were stronger than GDDsos-pos ($w = 0.37$–0.70, $p < 0.05$) (Fig. 6c). Additionally, CPsos-pos could positively impact the AGB in the temperate arid or semi-arid regions (HIIC2, meadow: $w = 0.64$, $p < 0.01$; steppe: $w = 0.73$, $p < 0.001$; HIID1, meadow: $w = 0.56$, $p < 0.05$; steppe: $w = 0.58$, $p < 0.05$). However, GDDsos-pos positively affected the AGB of meadows in both the temperate humid region (HIIA, $w = 0.51$, $p < 0.05$) and temperate semi-arid region (HIIC1, $w = 0.67$, $p < 0.01$) (Fig. 6d).

4. Discussion

4.1. Climate primarily impacts variation in alpine grasslands AGB through direct paths

At the regional scale, both direct and indirect paths (mediated by phenology) were identified for the impacts of climate on AGB. Predominantly, climatic accumulation directly impacted the AGB during preseason or growing season, whether in the sub-cold regions or temperate regions (Fig. 7). However, although the phenology-mediated path that climate indirectly affected the AGB did exist, the magnitude of the impact was weak (Fig. 7). Specifically, in the HIB region, the

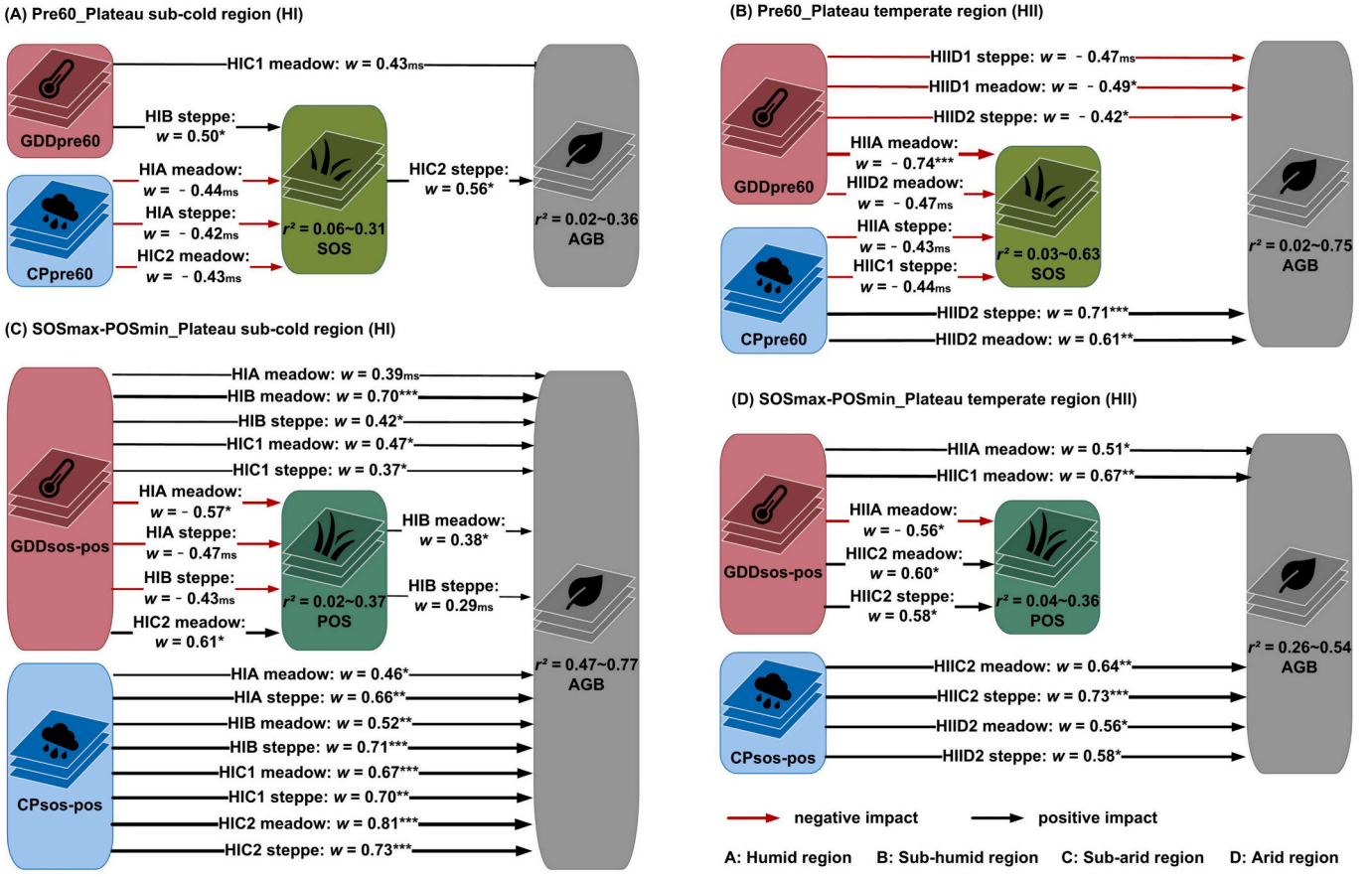

Fig. 6. Impact paths of water and heat accumulation on phenology and aboveground biomass in different climate zones. ("ms" indicates $p < 0.1$ (marginally significant), "*" indicates $0.1 \leq p < 0.05$, "**" indicates $p < 0.01$, "***" indicates $p < 0.001$. GDDpre60, growing degree-days in the preseason 60 days; CPpre60, cumulative precipitation in the preseason 60 days; GDDsos-pos, growing degree-days from SOS_{17max} to POS_{17min} (i.e., growing season); CPsos-pos, cumulative precipitation from SOS_{17max} to POS_{17min}. AGB, aboveground biomass; SOS, start date of the growing season; POS, peak date of the growing season). Here, all impact paths were synthesized, and the test of each path was shown in the Table S1 and Table S2.

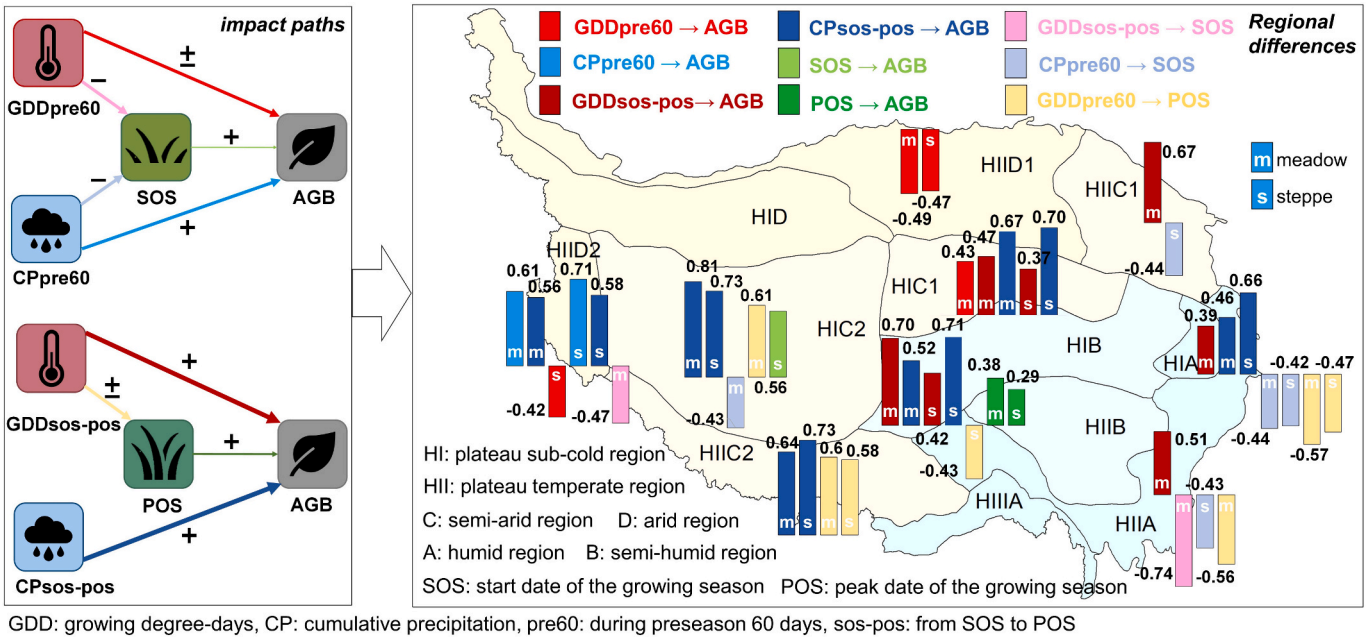

Fig. 7. Path coefficient partitioning map of climate affecting aboveground biomass in alpine grasslands across the Qinghai-Tibet Plateau.

GDDsos-pos initially negatively affected POS of alpine steppe, and then positively affected AGB. This finding is consistent with Yang et al. (2019a), who observed that delayed peak photosynthesis timing was associated with higher peak production in the QTP alpine grasslands. Additionally, a report across 36 stations on the QTP found that climate variables, especially growing season precipitation, had a greater impact on aboveground net primary productivity than phenological changes in alpine grasslands (Wang et al., 2022a). This is highly consistent with our study, where the impacts of cumulative precipitation during the growing season on AGB (w = 0.46–0.81) were stronger than did phenological changes (w = 0.29–0.38).

The regulatory effects of SOS and POS on AGB were not significant across most climate regions ($p > 0.1$) (Fig. 6), suggesting that the "growth carryover effect" didn't predominantly govern AGB accumulation at the regional scale in the QTP alpine grasslands during 2002 to 2018. Zheng et al. (2020) reported that the promoting effect of the SOS on summer net primary productivity (NPP) in alpine grasslands was less significant than spring NPP on the QTP. A majority of SOS pixels (65.9 %) showed an advancing trend, with 5.8 % of pixels advancing significantly by 0 to 1 day/year ($p < 0.05$) (Fig. S2c, Fig. S2d), leading to increased spring evapotranspiration. This advancement could deplete soil moisture sooner, exacerbating water limitations caused by summer drought on the QTP (Chen et al., 2022). Our findings demonstrated that CPsos-pos had direct and positive impacts on AGB in almost all climate regions ($p < 0.05$), indicating that the peak AGB accumulation was indeed negatively impacted by the drought during the growing season. On the other hand, the minimal regulatory effects of SOS on peak AGB implied a weak spring-summer linkage between SOS and vegetation biomass. This, combined with the direct positive impact of CPsos-pos on AGB, supports evidences for a discovery that vegetation in the northern hemisphere was gradually moving toward a "structural overshoot effect" from 2002 to 2021 (Lian et al., 2024).

4.2. Regional differences of climatic impact on AGB in alpine grasslands

By mapping the paths and degree across various climate regions (Fig. 6, Fig. 7), the study generalized three regional-difference patterns of impact paths (Fig. 8).

4.2.1. Pattern 1—In the plateau temperate arid regions, an increase in cumulative precipitation during the preseason 60 days (CPpre60) promoted AGB, whereas an increase in growing degree-days (GDDpre60) inhibited AGB (Fig. 8a, Fig. S5c, d)

Specifically, in the temperate arid region (HIID2), CPpre60 exerted positive effects on AGB. A study summarized two effects of "snow → vegetation productivity" in the Greater Himalaya ("→" indicate impact) (Wang et al., 2018a). One was the water-promoting effect of "snow $\overset{+}{\rightarrow}$ soil moisture $\overset{+}{\rightarrow}$ vegetation productivity", the second one was the phenology-promoting effect of "snow $\overset{+}{\rightarrow}$ melting date $\overset{+}{\rightarrow}$ spring phenology $\overset{+}{\rightarrow}$ vegetation productivity". Further, we found that in the plateau temperate arid region (HIID2), the increase in CPpre60 (snow cover) had a direct promoting effect on AGB in the two grassland types, which was related to the fact that snowmelt increased soil moisture in spring and summer, thereby promoted vegetation growth (Peng et al., 2010; Wang et al., 2018b), In fact, precipitation is one of the primary water sources required for the growth of alpine grasslands, and it carries nutrients from the atmosphere. Moreover, its seasonal variations directly influence the regulatory mechanisms of plant growth in alpine grasslands. Novelly, in the sub-cold region (HIC2), we also found positive regulation of SOS on AGB in the steppe, which was agreement with the phenology-promoting effect of Wang et al. (2018a). However, the increased GDDpre60 in the temperate arid regions (HIID1, HIID2) inhibited AGB, because the preseason high temperatures in these arid regions probably reduced water availability by increasing evapotranspiration, thereby reducing AGB accumulation in alpine grasslands.

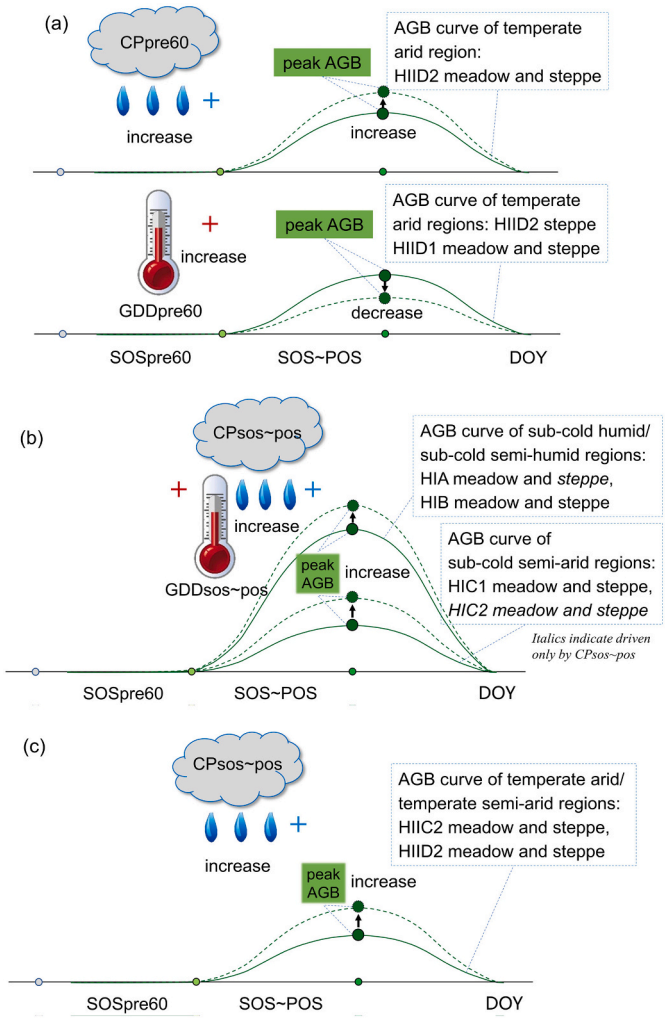

Fig. 8. Regional-difference patterns of climate impacts on AGB of alpine grasslands (a) In the plateau temperate arid regions (e.g., HIID1 or HIID2), the increase in CP during the preseason 60 days promoted AGB, while the increase in GDD during the preseason 60 days inhibited AGB. (b) In the plateau sub-cold regions, the increase in CP or GDD during the growing season could significantly promoted grasslands AGB, respectively. (c) In the plateau temperate arid/semi-arid regions (e.g., HIIC2 and HIID1), the increased in CP during the growing season significantly promoted the AGB. AGB, aboveground biomass; CP, cumulative precipitation; GDD, growing degree-days; POS, peak date of the growing season; SOS, start date of the growing season.

4.2.2. Pattern 2—In the plateau sub-cold regions, increases in cumulative precipitation or growing degree-days during the growing season (CPsos-pos or GDDsos-pos) could significantly promote grassland AGB, respectively (Fig. 8b)

Spatially, there was also an overall positive correlation between climate accumulation and AGB during the growing season in plateau sub-cold regions except for HIC2 for GDDsos-pos (Fig. S5e, f). On one hand, CPsos-pos positively affected AGB in the sub-cold regions ($p < 0.05$), which was supported by the results of site control experiments. For example, Fu et al. (2018) found that increased precipitation during the growing season had a greater impact on alpine meadow productivity than experimental warming at the Damxung Observatory (30°30′N, 91°04′E, located in the sub-cold semi-arid region HIC2). Additionally, climatic control experiment conducted at the Namtso Observatory (30°46′N, 90°59′E, semi-arid region HIC2) demonstrated that increased

precipitation and soil moisture during the growing season positively impacted alpine grassland AGB/GPP (Zhao et al., 2019; Wang et al., 2020b). In this study, at the regional scale, cumulative precipitation during the growing season in HIC2 had a highly significant positive impact on AGB in both alpine meadows and alpine steppes, while no significant effects of GDDsos-pos on AGB in alpine grasslands (HIC2) were detected (Fig. 6).

On the other hand, it was imperative to acknowledge the positive impact of GDDsos-pos on AGB in sub-cold regions. Specifically, the direct positive effects have been observed in sub-cold humid/semi-humid regions and semi-arid region (Fig. 6). It was reported that the average temperature of the QTP ranges from −2 to 0 °C (Shen et al., 2015). The optimal temperature for increasing productivity of alpine grasslands was 13 ± 3 °C, while the annual average maximum temperature was still slightly lower than this threshold (Huang et al., 2019), suggesting that the increased GDDsos-pos conceals the potential to enhance alpine grassland biomass/productivity. Additionally, in the temperate semi-arid region (HIIC1), increased GDDsos-pos could improve AGB in alpine meadows (Fig. 6d), consistent with the finding of Chen et al. (2016) that warming during the growing season could significantly increase AGB in an alpine meadow at Haibei Station (100°51′E, 36°57′N, HIIC1).

4.2.3. Pattern 3 - In the temperate arid or semi-arid regions (e.g., HIIC2 and HIID1), the increase in cumulative precipitation during the growing season (CPsos-pos) significantly promoted the AGB (Fig. 8c)

Correspondingly, Zha et al. (2022) also found that significant positive correlation between the average annual precipitation and grassland NPP in arid or semi-arid regions, especially for the water-deficient regions in the southwest of the QTP (e.g., HIIC2). In addition, Zhang et al. (2023c) found that the optimal time for water's impact on AGB in QTP alpine grasslands occurred approximately one month before the flowering period or the fruit maturity, which was congruent with the result that the cumulative precipitation during the growing season significantly affected AGB in this study.

4.3. Limitations and prospects

The climate variables in this study were focused on the temperature and precipitation. However, solar radiation can also affect biomass accumulation by influencing physiological processes in leaves (e.g., photosynthesis). It has been reported that variations in radiation play very important roles in regulating the potential forage nutritional quality and carbon storage in the QTP alpine grasslands (Fu et al., 2022; Li and Fu, 2023). Beyond climate drivers, factors such as topography, edaphic conditions, and human activities could also exert direct or indirect effects on the variability of AGB in alpine grasslands. For instance, the substantial elevation gradients across the QTP can profoundly affect the spatial and temporal variations in grassland biomass and phenology by redistributing water and heat resources (Wang et al., 2017). To some extent, climate regions can represent variations in water and heat availability that are attributable to rugged terrain and monsoon influences.

Additionally, this study did not consider the impacts of human disturbances, especially grazing intensity, on grassland AGB. A series of ecological restorations have been conducted on the QTP Since 2000, which have reduced human interferences and brought the grasslands closer to their original natural state (Li et al., 2021a). However, grazing remains the primary human activity affecting vegetation growth. There is ongoing debate regarding the relative contributions of climate factors and grazing activities to grassland productivity on the QTP (Chen et al., 2014; Li et al., 2021a; Wei et al., 2022; Zhou et al., 2024). Grazing activities have complex effects on the grassland ecosystem, varying across regions and periods. Therefore, in the future, it is crucial to explore the coupling mechanisms between human activities and natural factors affecting grassland biomass, including the direct and indirect effects on changes in AGB.

Biological factors, such as community composition and growth rate, may also modulate variations in grassland AGB (Wang et al., 2020a). However, effectively quantifying these factors at a regional scale remains a significant challenge. In addition, this study primarily focused on the impacts of preseason and spring-summer climatic factors on peak AGB. Nevertheless, considering the full lifecycle of alpine grasslands, further investigation is necessary to understand the lagged effects of post-growing season climate (from POS to EOS) on the next year's SOS and AGB. A study reported that significant positive effects of previous year's precipitation on current AGB in control experiments on the Chinese Loess Plateau (Gong et al., 2020).

Remarkably, in path analysis, using the regional averages of climatic and phenological variables can reflect the overall characteristic of each climatic region, which provide the result of equilibrium state and is not disproportionately affected by anomalous data. Even so, due to differences in influencing factors, scale effects and spatial heterogeneity, regional averages still may not fully align with analysis results from individual pixels or sites.

5. Conclusions

Using the observed aboveground biomass (peak AGB) data, remote sensing and high-precision climate data in alpine grasslands across the Qinghai-Tibet Plateau during 2002–2018, this study systematically analyzed the regional differences in the impact paths of climate on peak AGB by dividing the phenophases and climate regions. During the preseason and especially the growing season, water and heat accumulation mostly directly impacted the AGB through direct paths, whether in the plateau sub-cold regions or temperate regions. Although a phenology-mediated path through which climate indirectly affected AGB was identified, its impact was relatively weak. The weak spring-summer linkage between SOS and AGB, combined with direct and positive impacts of cumulative precipitation, provides evidence that alpine grasslands have gradually moved toward a “structural overshoot effect” during 2002–2018. With increasing drought severity, general characteristics showed declines or delays in AGB, water and heat accumulation (except for GDDpre60), SOS and POS. The regional-difference patterns were summarized as follows: In plateau temperate arid regions, preseason water and heat accumulation exerted opposite impacts on AGB, whereas in plateau sub-cold regions, these factors consistently enhanced AGB during the growing season. Likewise, in plateau temperate arid or semi-arid regions, cumulative precipitation during the growing season also showed a strong positive effect on AGB. The study identified diverse impacts and regional differences of water and heat accumulation on AGB by dividing different phenophases and climatic regions. This is highly significant for the spatial planning and management of alpine grasslands, and for understanding the mechanisms and trends of grassland biomass variations under rapid climate change.

CRediT authorship contribution statement

Peixian Li: Writing – review & editing, Writing – original draft, Visualization, Software, Methodology, Funding acquisition, Formal analysis, Data curation, Conceptualization. **Wenquan Zhu:** Writing – review & editing, Supervision, Resources, Methodology, Funding acquisition, Formal analysis, Conceptualization. **Bangke He:** Software, Methodology, Data curation.

Declaration of competing interest

The authors declare that they have no known competing financial interests or personal relationships that could have appeared to influence the work reported in this paper.

Data availability

Data will be made available on request.

Acknowledgements

This work was supported by the National Natural Science Foundation of China (Grant No. 41771047) and Scientific Research Fund of the Fourth Institute of Oceanography, Ministry of Natural Resources (Grant No. JKF202303).

Appendix A. Supplementary data

Supplementary data to this article can be found online at https://doi.org/10.1016/j.scitotenv.2024.174421.

References

Bai, Y., Cotrufo, M.F., 2022. Grassland soil carbon sequestration: current understanding, challenges, and solutions. Science 377 (6606), 603–608. https://doi.org/10.1126/science.abo2380.

Chen, B., Zhang, X., Tao, J., Wu, J., Wang, J., Shi, P., Zhang, Y., Yu, C., 2014. The impact of climate change and anthropogenic activities on alpine grassland over the Qinghai-Tibet Plateau. Agric. For. Meteorol. 189, 11–18. https://doi.org/10.1016/j.agrformet.2014.01.002.

Chen, J., Luo, Y., Xia, J., Shi, Z., Jiang, L., Niu, S., Zhou, X., Cao, J., 2016. Differential responses of ecosystem respiration components to experimental warming in a meadow grassland on the Tibetan Plateau. Agric. For. Meteorol. 220, 21–29. https://doi.org/10.1016/j.agrformet.2016.01.010.

Chen, F., Fu, B., Xia, J., Al, E., 2019. Major advances in studies of the physical geography and living environment of China during the past 70 years and future prospects. Sci. China Earth Sci. 49, 1659–1696 (in Chinese). https://doi.org/10.1360/sste-2019-0174.

Chen, N., Zhang, Y., Song, C., Xu, M., Zhang, T., Li, M., Cong, N., Zu, J., Zheng, Z., Ma, G., Huang, K., 2022. The chained effects of earlier vegetation activities and summer droughts on ecosystem productivity on the Tibetan Plateau. Agric. For. Meteorol. 321, 108975 https://doi.org/10.1016/j.agrformet.2022.108975.

Diao, C., Liu, Y., Zhao, L., Zhuo, G., Zhang, Y., 2021. Regional-scale vegetation-climate interactions on the Qinghai-Tibet Plateau. Eco. Inform. 65, 101413 https://doi.org/10.1016/j.ecoinf.2021.101413.

Dong, S., Shang, Z., Gao, J., Boone, R.B., 2020. Enhancing sustainability of grassland ecosystems through ecological restoration and grazing management in an era of climate change on Qinghai-Tibetan Plateau. Agr Ecosyst Environ 287, 106684. https://doi.org/10.1016/j.agee.2019.106684.

Du, Q., Sun, Y., Guan, Q., Pan, N., Wang, Q., Ma, Y., Li, H., Liang, L., 2022. Vulnerability of grassland ecosystems to climate change in the Qilian Mountains, northwest China. J. Hydrol. 612, 128305 https://doi.org/10.1016/j.jhydrol.2022.128305.

Editorial Board of Vegetation Map of China Cas, 2001. In: Hou, X.Y. (Ed.), 1:1000,000 Vegetation Atlas of China. Science Press, Beijing, China.

Fang, J., Ke, J., Tang, Z., Chen, A., 2001. Implications and estimations of four terrestrial productivity parameters (in Chinese). Acta Phytoecologica Sin. 25, 414–419.

Fayiah, M., Dong, S.K., Khomera, S.W., Rehman, S.A.U., Yang, M., Xiao, J., 2020. Status and challenges of Qinghai-Tibet Plateau's grasslands: an analysis of causes, mitigation measures, and way forward. Sustainability 12, 1–12. https://doi.org/10.3390/su12031099.

Fu, Y.H., Piao, S., Zhao, H., Jeong, S.J., Wang, X., Vitasse, Y., Ciais, P., Janssens, I.A., 2014. Unexpected role of winter precipitation in determining heat requirement for spring vegetation green-up at northern middle and high latitudes. Glob. Chang. Biol. 20, 3743–3755. https://doi.org/10.1111/gcb.12610.

Fu, G., Shen, Z.X., Zhang, X.Z., 2018. Increased precipitation has stronger effects on plant production of an alpine meadow than does experimental warming in the Northern Tibetan Plateau. Agric. For. Meteorol. 249, 11–21. https://doi.org/10.1016/j.agrformet.2017.11.017.

Fu, G., Wang, J., Li, S., 2022. Response of forage nutritional quality to climate change and human activities in alpine grasslands. Sci. Total Environ. 845, 157552 https://doi.org/10.1016/j.scitotenv.2022.157552.

Ganjurjav, H., Gornish, E., Hu, G., Wu, J., Wan, Y., Li, Y., Gao, Q., 2021. Phenological changes offset the warming effects on biomass production in an alpine meadow on the Qinghai–Tibetan Plateau. J. Ecol. 109, 1014–1025. https://doi.org/10.1111/1365-2745.13531.

Gong, Y.H., Zhao, D.M., Ke, W.B., Fang, C., Pei, J.Y., Sun, G.J., Ye, J.S., 2020. Legacy effects of precipitation amount and frequency on the aboveground plant biomass of a semi-arid grassland. Sci. Total Environ. 705, 135899 https://doi.org/10.1016/j.scitotenv.2019.135899.

Gonsamo, A., Chen, J.M., Ooi, Y.W., 2018. Peak season plant activity shift towards spring is reflected by increasing carbon uptake by extratropical ecosystems. Glob. Chang. Biol. 24, 2117–2128. https://doi.org/10.1111/gcb.14001.

He, J., Yang, K., Tang, W., Lu, H., Qin, J., Chen, Y., Li, X., 2020. The first high-resolution meteorological forcing dataset for land process studies over China. Sci. Data 7, 1–11. https://doi.org/10.1038/s41597-020-0369-y.

Hoffmann, A.A., Camac, J.S., Williams, R.J., Papst, W., Jarrad, F.C., Wahren, C.H., 2010. Phenological changes in six Australian subalpine plants in response to experimental warming and year-to-year variation. J. Ecol. 98, 927–937. https://doi.org/10.1111/j.1365-2745.2010.01667.x.

Hossain, M.L., Li, J., 2020. Effects of long-term climatic variability and harvest frequency on grassland productivity across five ecoregions. Global Ecol. Conserv. 23, 1–19. https://doi.org/10.1016/j.gecco.2020.e01154.

Huang, M., Piao, S., Ciais, P., Peñuelas, J., Wang, X., Keenan, T.F., Peng, S., Berry, J.A., Wang, K., Mao, J., Alkama, R., Cescatti, A., Cuntz, M., De Deurwaerder, H., Gao, M., He, Y., Liu, Y., Luo, Y., Myneni, R.B., Niu, S., Shi, X., Yuan, W., Verbeeck, H., Wang, T., Wu, J., Janssens, I.A., 2019. Air temperature optima of vegetation productivity across global biomes. Nat. Ecol. Evol. 3, 772–779. https://doi.org/10.1038/s41559-019-0838-x.

Jolly, W.M., Nemani, R., Running, S.W., 2005. A generalized, bioclimatic index to predict foliar phenology in response to climate. Glob. Chang. Biol. 11, 619–632. https://doi.org/10.1111/j.1365-2486.2005.00930.x.

Jump, A.S., Ruiz-Benito, P., Greenwood, S., Allen, C.D., Kitzberger, T., Fensham, R., Martínez-Vilalta, J., Lloret, F., 2017. Structural overshoot of tree growth with climate variability and the global spectrum of drought-induced forest dieback. Glob. Chang. Biol. 23, 3742–3757. https://doi.org/10.1111/gcb.13636.

Knapp, A.K., Smith, M.D., 2001. Variation among biomes in temporal dynamics of aboveground primary production. Science 291, 481–484. https://doi.org/10.1126/science.291.5503.481.

Koebsch, F., Sonnentag, O., Järveoja, J., Peltoniemi, M., Alekseychik, P., Aurela, M., Arslan, A.N., Dinsmore, K., Gianelle, D., Helfter, C., Jackowicz-Korczynski, M., Korrensalo, A., Leith, F., Linkosalmi, M., Lohila, A., Lund, M., Maddison, M., Mammarella, I., Mander, Ü., Minkkinen, K., Pickard, A., Pullens, J.W.M., Tuittila, E. S., Nilsson, M.B., Peichl, M., 2020. Refining the role of phenology in regulating gross ecosystem productivity across European peatlands. Glob. Chang. Biol. 26, 876–887. https://doi.org/10.1111/gcb.14905.

Lefcheck, J.S., 2016. piecewiseSEM: piecewise structural equation modelling in r for ecology, evolution, and systematics. Methods Ecol. Evol. 7, 573–579. https://doi.org/10.1111/2041-210X.12512.

Li, W., 2017. An overview of ecological research conducted on the Qinghai-Tibetan Plateau. J. Resour. Ecol. 8, 1–4. https://doi.org/10.5814/j.issn.1674-764x.2017.01.001.

Li, S., Fu, G., 2023. Impacts of anthropogenic activities and climate change on forage nutrition storage in Tibetan grasslands. Plants 12 (14), 2735. https://doi.org/10.3390/plants12142735.

Li, L., Zhang, Y., Wu, J., Li, S., Zhang, B., Zu, J., Zhang, H., Ding, M., Paudel, B., 2019. Increasing sensitivity of alpine grasslands to climate variability along an elevational gradient on the Qinghai-Tibet Plateau. Sci. Total Environ. 678, 21–29. https://doi.org/10.1016/j.scitotenv.2019.04.399.

Li, J., Wu, C., Wang, X., Peng, J., Dong, D., Lin, G., Gonsamo, A., 2020. Satellite observed indicators of the maximum plant growth potential and their responses to drought over Tibetan Plateau (1982–2015). Ecol. Indic. 108, 105732 https://doi.org/10.1016/j.ecolind.2019.105732.

Li, M., Wu, J., Feng, Y., Niu, B., He, Y., Zhang, X., 2021a. Climate variability rather than livestock grazing dominates changes in alpine grassland productivity across Tibet. Front. Ecol. Evol. 9, 631024 https://doi.org/10.3389/fevo.2021.631024.

Li, P., Zhu, W., Xie, Z., 2021b. Diverse and divergent influences of phenology on herbaceous aboveground biomass across the Tibetan Plateau alpine grasslands. Ecol. Indic. 121, 107036 https://doi.org/10.1016/j.ecolind.2020.107036.

Lian, X., Piao, S., Chen, A., Wang, K., Li, X., Buermann, W., Huntingford, C., Peñuelas, J., Xu, H., Myneni, R.B., 2021. Seasonal biological carryover dominates northern vegetation growth. Nat. Commun. 12 https://doi.org/10.1038/s41467-021-21223-2.

Lian, X., Peñuelas, J., Ryu, Y., Piao, S., Keenan, T.F., Fang, J., Yu, K., Chen, A., 2024. Diminishing carryover benefits of earlier spring vegetation growth. Nat. Ecol. Evol. https://doi.org/10.1038/s41559-023-02272-w.

Liu, X., Chen, B., 2000. Climatic warming in the Tibetan Plateau during recent decades. Int. J. Climatol. 20 (14), 1729–1742. https://doi.org/10.1002/1097-0088(20001130)20:14<1729::AID-JOC556>3.0.CO;2-Y.

Ma, R., Xia, C., Liu, Y., Wang, Y., Zhang, J., Shen, X., Lu, X., Jiang, M., 2022. Spatiotemporal change of net primary productivity and its response to climate change in temperate grasslands of China. Front. Plant Sci. 13 https://doi.org/10.3389/fpls.2022.899800.

Michaletz, S.T., Cheng, D., Kerkhoff, A.J., Enquist, B.J., 2014. Convergence of terrestrial plant production across global climate gradients. Nature 512, 39–43. https://doi.org/10.1038/nature13470.

Ogle, K., Barber, J.J., Barron-Gafford, G.A., Bentley, L.P., Young, J.M., Huxman, T.E., Loik, M.E., Tissue, D.T., 2015. Quantifying ecological memory in plant and ecosystem processes. Ecol. Lett. 18, 221–235. https://doi.org/10.1111/ele.12399.

O'Mara, F.P., 2012. The role of grasslands in food security and climate change. Ann. Bot. 110, 1263–1270. https://doi.org/10.1093/aob/mcs209.

Peng, S., Piao, S., Ciais, P., Fang, J., Wang, X., 2010. Change in winter snow depth and its impacts on vegetation in China. Glob. Chang. Biol. 16, 3004–3013. https://doi.org/10.1111/j.1365-2486.2010.02210.x.

Piao, S., Fang, J., Zhou, L., Ciais, P., Zhu, B., 2006. Variations in satellite-derived phenology in China's temperate vegetation. Glob. Chang. Biol. 12, 672–685. https://doi.org/10.1111/j.1365-2486.2006.01123.x.

Rehling, F., Sandner, T.M., Matthies, D., 2021. Biomass partitioning in response to intraspecific competition depends on nutrients and species characteristics: a study of 43 plant species. J. Ecol. 109, 2219–2233. https://doi.org/10.1111/1365-2745.13635.

Robinson, T.M.P., La Pierre, K.J., Vadeboncoeur, M.A., Byrne, K.M., Thomey, M.L., Colby, S.E., 2013. Seasonal, not annual precipitation drives community productivity across ecosystems. Oikos 122, 727–738. https://doi.org/10.1111/j.1600-0706.2012.20655.x.

Scurlock, J.M.O., Hall, D.O., 1998. The global carbon sink: a grassland perspective. Glob. Chang. Biol. 4, 229–233. https://doi.org/10.1046/j.1365-2486.1998.00151.x.

Shen, M., Piao, S., Cong, N., Zhang, G., Jassens, I.A., 2015. Precipitation impacts on vegetation spring phenology on the Tibetan Plateau. Glob. Chang. Biol. 21, 3647–3656. https://doi.org/10.1111/gcb.12961.

Shipley, B., 2000. A new inferential test for path models based on directed acyclic graphs. Struct. Equ. Model. 7, 206–218. https://doi.org/10.1080/10705510903008279.

Sun, H., Chen, Y., Xiong, J., Ye, C., Yong, Z., Wang, Y., He, D., Xu, S., 2022. Relationships between climate change, phenology, edaphic factors, and net primary productivity across the Tibetan Plateau. Int. J. Appl. Earth Obs. Geoinf. 107, 102708 https://doi.org/10.1016/j.jag.2022.102708.

Wang, X., Chen, R., 2023. Evaluation of spatial and temporal variations in the difference between soil and air temperatures on the Qinghai–Tibetan plateau using reanalysis data products. Remote Sens. (Basel) 15 (7), 1894. https://doi.org/10.3390/rs15071894.

Wang, S., Zhang, B., Yang, Q., Chen, G., Yang, B., Lu, L., Shen, M., Peng, Y., 2017. Responses of net primary productivity to phenological dynamics in the Tibetan Plateau, China. Agric. For. Meteorol. 232, 235–246. https://doi.org/10.1016/j.agrformet.2016.08.020.

Wang, Xiaoyi, Wang, T., Guo, H., Liu, D., Zhao, Y., Zhang, T., Liu, Q., Piao, S., 2018a. Disentangling the mechanisms behind winter snow impact on vegetation activity in northern ecosystems. Glob. Chang. Biol. 24, 1651–1662. https://doi.org/10.1111/gcb.13930.

Wang, Xiaoyue, Wu, C., Peng, D., Gonsamo, A., Liu, Z., 2018b. Snow cover phenology affects alpine vegetation growth dynamics on the Tibetan Plateau: satellite observed evidence, impacts of different biomes, and climate drivers. Agric. For. Meteorol. 256–257, 61–74. https://doi.org/10.1016/j.agrformet.2018.03.004.

Wang, H., Liu, H., Cao, G., Ma, Z., Li, Y., Zhang, F., Zhao, Xia, Zhao, Xinquan, Jiang, L., Sanders, N.J., Classen, A.T., He, J.S., 2020a. Alpine grassland plants grow earlier and faster but biomass remains unchanged over 35 years of climate change. Ecol. Lett. 23, 701–710. https://doi.org/10.1111/ele.13474.

Wang, Y., Zhu, Z., Ma, Y., Yuan, L., 2020b. Carbon and water fluxes in an alpine steppe ecosystem in the Nam co area of the Tibetan Plateau during two years with contrasting amounts of precipitation. Int. J. Biometeorol. 64, 1183–1196. https://doi.org/10.1007/s00484-020-01892-2.

Wang, Y., Shen, X., Jiang, M., Tong, S., Lu, X., 2021. Spatiotemporal change of aboveground biomass and its response to climate change in marshes of the Tibetan Plateau. Int. J. Appl. Earth Obs. Geoinf. 102, 102385 https://doi.org/10.1016/j.jag.2021.102385.

Wang, J., Li, M., Yu, C., Fu, G., 2022a. The change in environmental variables linked to climate change has a stronger effect on aboveground net primary productivity than does phenological change in alpine grasslands. Front. Plant Sci. 12, 798633 https://doi.org/10.3389/fpls.2021.798633.

Wang, Y., Lv, W., Xue, K., Wang, S., Zhang, L., Hu, R., Zeng, H., Xu, X., Li, Y., Jiang, L., Hao, Y., Du, J., Sun, J., Dorji, T., Piao, S., Wang, C., Luo, C., Zhang, Z., Chang, X., Zhang, M., Hu, Y., Wu, T., Wang, J., Li, B., Liu, P., Zhou, Y., Wang, A., Dong, S., Zhang, X., Gao, Q., Zhou, H., Shen, M., Wilkes, A., Miehe, G., Zhao, X., Niu, H., 2022b. Grassland changes and adaptive management on the Qinghai–Tibetan Plateau. Nat. Rev. Earth Environ. 3, 668–683. https://doi.org/10.1038/s43017-022-00330-8.

Wei, Y., Lu, H., Wang, J., Wang, X., Sun, J., 2022. Dual influence of climate change and anthropogenic activities on the spatiotemporal vegetation dynamics over the Qinghai-Tibetan plateau from 1981 to 2015. Earth's Future 10 (5), e2021EF002566. https://doi.org/10.1029/2021EF002566.

Weiher, E., Werf, A., Thompson, K., Roderick, M., Garnier, E., Eriksson, O., 1999. Challenging Theophrastus: a common core list of plant traits for functional ecology. J. Veg. Sci. 10, 609–620. https://doi.org/10.2307/3237076.

Wen, Y., Liu, X., Xin, Q., Wu, J., Xu, X., Pei, F., Li, X., Du, G., Cai, Y., Lin, K., Yang, J., Wang, Y., 2019. Cumulative effects of climatic factors on terrestrial vegetation growth. J. Geophys. Res. Biogeo. 124, 789–806. https://doi.org/10.1029/2018JG004751.

Wu, K., Chen, J., Yang, H., Yang, Y., Hu, Z., 2023. Spatiotemporal variations in the sensitivity of vegetation growth to typical climate factors on the Qinghai–Tibet Plateau. Remote Sens. (Basel) 15. https://doi.org/10.3390/rs15092355.

Xie, Z., Zhu, W., He, B., Qiao, K., Zhan, P., Huang, X., 2022. A background-free phenology index for improved monitoring of vegetation phenology. Agric. For. Meteorol. 315, 108826 https://doi.org/10.1016/j.agrformet.2022.108826.

Yang, J., Dong, J., Xiao, X., Dai, J., Wu, C., Xia, J., Zhao, G., Zhao, M., Li, Z., Zhang, Y., Ge, Q., 2019a. Divergent shifts in peak photosynthesis timing of temperate and alpine grasslands in China. Remote Sens. Environ. 233, 111395 https://doi.org/10.1016/j.rse.2019.111395.

Yang, W., Kobayashi, H., Wang, C., Shen, M., Chen, J., Matsushita, B., Tang, Y., Kim, Y., Bret-Harte, M.S., Zona, D., Oechel, W., Kondoh, A., 2019b. A semi-analytical snow-free vegetation index for improving estimation of plant phenology in tundra and grassland ecosystems. Remote Sens. Environ. 228, 31–44. https://doi.org/10.1016/j.rse.2019.03.028.

You, Y., Wang, S., Pan, N., Ma, Y., Liu, W., 2020. Growth stage-dependent responses of carbon fixation process of alpine grasslands to climate change over the Tibetan Plateau, China. Agric. For. Meteorol. 291, 108085 https://doi.org/10.1016/j.agrformet.2020.108085.

Zha, X., Niu, B., Li, M., Duan, C., 2022. Increasing impact of precipitation on alpine-grassland productivity over last two decades on the Tibetan Plateau. Remote Sens. (Basel) 14, 1–14. https://doi.org/10.3390/rs14143430.

Zhai, D., Gao, X., Li, B., Yuan, Y., Jiang, Y., Liu, Y., Li, Y., Li, R., Liu, W., Xu, J., 2022. Driving climatic factors at critical plant developmental stages for Qinghai–Tibet Plateau Alpine grassland productivity. Remote Sens. (Basel) 14, 1–20. https://doi.org/10.3390/rs14071564.

Zhang, Y., Li, B., Zheng, D., 2002. A discussion on the boundary and area of the Tibetan Plateau in China (in Chinese). Geogr. Res. 21, 1–8.

Zhang, Y., Zhu, Y., Li, J., Chen, Y., 2019. Current status and future directions of the Tibetan Plateau ecosystem research. Sci. Bull. 64, 428–430. https://doi.org/10.1016/j.scib.2019.03.009.

Zhang, L., Gao, L., Chen, J., Zhao, L., Zhao, J., Qiao, Y., Shi, J., 2022. Comprehensive evaluation of mainstream gridded precipitation datasets in the cold season across the Tibetan Plateau. J. Hydrol.: Reg. Stud. 43, 101186 https://doi.org/10.1016/j.ejrh.2022.101186.

Zhang, C., Qin, D.H., Zhai, P.M., 2023a. Amplification of warming on the Tibetan Plateau. Adv. Clim. Chang. Res. 14 (4), 493–501. https://doi.org/10.1016/j.accre.2023.07.004.

Zhang, H., Tang, Z., Wang, B., Kan, H., Sun, Y., Qin, Y., Meng, B., Li, M., Chen, J., Lv, Y., Zhang, J., Niu, S., Yi, S., 2023b. A 250 m annual alpine grassland AGB dataset over the Qinghai-Tibet Plateau (2000-2019) in China based on in situ measurements, UAV photos, and MODIS data. Earth Syst. Sci. Data 15, 821–846. https://doi.org/10.5194/essd-15-821-2023.

Zhang, Y., Zhou, T., Liu, X., Zhang, J., Xu, Y., Zeng, J., Wu, X., Lin, Q., 2023c. Crucial roles of the optimal time-scale of water condition on grassland biomass estimation on Qinghai–Tibet Plateau. Sci. Total Environ. 905, 1–15. https://doi.org/10.1016/j.scitotenv.2023.167210.

Zhao, J., Luo, T., Wei, H., Deng, Z., Li, X., Li, R., Tang, Y., 2019. Increased precipitation offsets the negative effect of warming on plant biomass and ecosystem respiration in a Tibetan alpine steppe. Agric. For. Meteorol. 279 https://doi.org/10.1016/j.agrformet.2019.107761.

Zheng, J., Yin, Y., Li, B., 2010. A new scheme for climate regionalization in China (in Chinese). Acta Geograph. Sin. 65, 3–12.

Zheng, Z., Zhu, W., Zhang, Y., 2020. Direct and lagged effects of spring phenology on net primary productivity in the alpine grasslands on the Tibetan Plateau. Remote Sens. (Basel) 12, 1–14. https://doi.org/10.3390/rs12071223.

Zhou, W., Wang, T., Xiao, J., Wang, K., Yu, W., Du, Z., Yue, T., 2024. Grassland productivity increase was dominated by climate in Qinghai-Tibet Plateau from 1982 to 2020. J. Clean. Prod. 434, 140144 https://doi.org/10.1016/j.jclepro.2023.140144.

Zhu, W., He, B., Xie, Z., Zhao, C., Zhuang, H., Li, P., 2022. Reconstruction of vegetation index time series based on self-weighting function fitting from curve features. Remote Sens. (Basel) 14, 1–18. https://doi.org/10.3390/rs14092247.